Title

GFI1 downregulation promotes inflammation-linked metastasis of colorectal cancer.

Journal

Cell death and differentiation, 24(5)

ISSN

1350-9047

Authors

Xing, Wenjing
Xiao, Yun
Lu, Xinliang
et al.

Publication Date

2017-05-01

DOI

10.1038/cdd.2017.50

Peer reviewed

OPEN

Cell Death and Differentiation (2017) 24, 929–943
Official journal of the Cell Death Differentiation Association

www.nature.com/cdd

GFI1 downregulation promotes inflammation-linked metastasis of colorectal cancer

Wenjing Xing[1,2,7], Yun Xiao[3,7], Xinliang Lu[1,2,4], Hongyan Zhu[1,2], Xiangchuan He[1,2], Wei Huang[1,2], Elsa S Lopez[5], Jerry Wong[5], Huanyu Ju[1,2], Linlu Tian[1,2], Fengmin Zhang[2], Hongwei Xu[1,2], Sheng Dian Wang[4], Xia Li[*,3], Michael Karin[*,5] and Huan Ren[*,1,2,6]

Inflammation is frequently associated with initiation, progression, and metastasis of colorectal cancer (CRC). Here, we unveil a CRC-specific metastatic programme that is triggered via the transcriptional repressor, GFI1. Using data from a large cohort of clinical samples including inflammatory bowel disease and CRC, and a cellular model of CRC progression mediated by cross-talk between the cancer cell and the inflammatory microenvironment, we identified GFI1 as a gating regulator responsible for a constitutively activated signalling circuit that renders CRC cells competent for metastatic spread. Further analysis of mouse models with metastatic CRC and human clinical specimens reinforced the influence of GFI1 downregulation in promoting CRC metastatic spread. The novel role of GFI1 is uncovered for the first time in a human solid tumour such as CRC. Our results imply that GFI1 is a potential therapeutic target for interfering with inflammation-induced CRC progression and spread.
Cell Death and Differentiation (2017) **24,** 929–943; doi:10.1038/cdd.2017.50; published online 7 April 2017

Chronic inflammation is an important risk factor for colorectal cancer (CRC) development and progression.[1–3] Colitis-associated CRC shows more rapid progression, lower sensitivity to treatment and higher mortality than sporadic CRC.[4] The tumour microenvironment contains cytokines, chemokines, inflammatory mediators, and so on, which have critical roles in almost every stage of progression to malignancy and metastasis.[5–11] Approximately 50% of CRC patients develop metastatic disease, and only a minority of patients who undergo resection of metastases attain long-term survival.[12]

CRC progression to metastatic disease is a multi-step process involving extensive tumour–stroma cross-talk. Potent metastasis-promoting factors, including cytokines and extracellular matrix (ECM) proteins, may trigger epithelial mesenchymal transition (EMT), which drives cancer cell dissemination. ECM-degrading proteases and the c-MET, Notch, and TGFβ signalling pathways regulate tumour–stroma interactions and metastasis.[13–15] Among these, TGFβ signalling is essential for the metastasis of CRC cells. Mice treated with a TGFβR1 inhibitor were resilient to metastasis formation.[15] Within the tumour microenvironment, amplified cyclo-oxygenase (COX)-converted prostaglandin E_2 (PGE_2) further induces the secretion of IL6, IL8, VEGF, iNOS, MMP-2, and MMP-9, leading to increased tumour invasion and metastasis.[16] PGE_2 exerts its effect by binding to EP receptors. Recent studies have shown that PGE_2–EP2 signalling in tumour-infiltrating neutrophils promotes CRC cell growth via amplifying inflammation and shaping the tumour microenvironment.[17,18] Moreover, tumour-associated macrophages (TAMs) are a major component promoting cancer progression in many aspects. The association between high TAMs and poor prognosis is observed in CRC.[6] Nevertheless, tumour–stroma cross-talk during metastatic progression is highly complex, and the signalling events that control metastasis may be stage-specific. Eventually, potent microenvironmental factors may initiate a programme in which responsive cancer cells are selected as metastatic initiators that may travel to a secondary site and establish metastatic growth.[19]

Transcription factors (TF) have key roles in determining cell fate and behaviour. Given a significant link between inflammatory bowel disease (IBD) and CRC,[20] we aimed to define key TF-regulated networks that may mediate transition programmes during CRC progression by analysing data sets from a large cohort of clinical specimens (Supplementary Figure S1).[21] We thus defined a 24-core TF-regulated network comprising inflammation- and/or CRC-related genes.[21] To validate the TF network in a cellular model, we applied an inflammation-promoting culture medium,[22] LSMCM (LPS-stimulated Monocyte Conditioned Medium), derived from human THP1 cells, to a series of CRC cell lines (Supplementary Figure S2A). LSMCM exposure triggered changes in CRC cell behaviour, including the EMT, and greatly increased cell migration and invasion.[21] The expression of two

[1]Department of Immunology, Harbin Medical University, Harbin 150081, China; [2]Immunity & Infection Key laboratory of Heilongjiang Province, Harbin 150081, China; [3]Department of Bioinformatics, College of Bioinformatics, Harbin Medical University, Harbin 150081, China; [4]Center of Infection and Immunity, Institute of Biophysics, Chinese Academy of Sciences, Beijing, China; [5]Laboratory of Gene Regulation and Signal Transduction, Departments of Pharmacology and Pathology, School of Medicine, University of California, San Diego, 9500 Gilman Drive, La Jolla, CA, 92093, USA and [6]College of basic medicine, Shanghai University Of Medicine & Health Sciences, Shanghai 201318, China

*Corresponding author: H Ren, Department of Immunology, Harbin Medical University, 157 Baojian Road, room409, Molecular&Biology Building, Harbin, 150081, China. Tel: +86 451 86674566; Fax: +86 451 86697322; E-mail: huanren2009@126.com

or M Karin, Laboratory of Gene Regulation and Signal Transduction, Departments of Pharmacology and Pathology, School of Medicine, University of California, San Diego, 9500 Gilman Drive, La Jolla, CA, 92093, USA. Tel: +858 534 1361; Fax: +858 534 8158, E-mail: karinoffice@ucsd.edu

or X Li, College of Bioinformatics, Harbin Medical University, 157 Baojian Road, Harbin, 150081, China. Tel: +86 451 86695922; Fax: +86669617; E-mail: lixia@hrbmu.edu.cn

[7]These authors contributed equally to this work.

Received 22.7.16; revised 27.2.17; accepted 06.3.17; Edited by G Melino; published online 07.4.2017

TFs, including GFI1 (Growth factor independence 1) and STAT3, was significantly altered after LSMCM application (Supplementary Figure S1B and Table 1).

GFI1 is a six-zinc-finger transcription repressor belonging to the SNAG domain family.[23] GFI1 has primarily been examined for its roles in different haematopoietic compartments,[24,25] cell cycle regulation,[23] and haematopoiesis.[26–29] Outside of the haematopoietic system, GFI1 is involved in lineage decisions during intestinal epithelial cell (IEC) differentiation.[30,31] Until recently, however, it is not known whether GFI1 contributes to CRC development and progression. Here, we described the establishment of a constitutively activated feed-forward inflammatory signalling circuit normally harnessed through GFI1 during CRC progression. This circuit has crucial roles in promoting CRC metastatic spread.

Results

Monocyte-derived TGF*β* induces inflammation-linked CRC cell metastatic behaviours. We generated a previously established cellular model using LSMCM culture medium conditioned by LPS-stimulated monocytes (Supplementary Figure S2A).[21,22] Four (HT29, LoVo, HCT116, and SW480) of the five CRC cell lines (including SW620) actively responded to LSMCM, morphologically changing into spindle-shaped fibroblast-like cells (Figure 1a). Further examination revealed that LSMCM greatly induced EMT and increased cell migration and invasion in responsive cells (Figure 1b–i and Supplementary Figure S2B); however, SW620 cells were the least responsive to LSMCM (Figure 1j and k), in which remnant LPS had a minor effect (Supplementary Figure S2C). Moreover, the conditioned medium derived from LPS-stimulated macrophages differentiated from human peripheral blood mononuclear cells (PBMCs), or the U-937 human monocyte cell line significantly induced EMT and increased cell migration and invasion in HT29 cells (Supplementary Figure S2D–F). These supplementary models provided proof of concept on the cellular model system to study the effect of TAMs and the tumour microenvironment *in vitro*.

To understand how LSMCM elicited these phenotypic changes, we analysed the supernatants of LSMCM-stimulated HT29 cells on 40 selected cytokines highly relevant to activated macrophages.[32] The results indicated that the concentrations of TGF*β*1, IL1*α*, IFN*γ*, I309 (CCL1), and TNF*β* were significantly decreased within the first 6 h of treatment and subsequently returned to levels equivalent to those present in the original LMSCM after 24 h of incubation, whereas GM-CSF, IL8, MCP1, PDGFBB, and sTNFR1 remained elevated for up to 24 h (Figure 2a). These data suggested that HT29 cells may consume or degrade certain cytokines in the medium before secreting these cytokines; these cells rapidly produced additional GM-CSF and IL8.

To identify the most important factors in LSMCM-affecting CRC cell behaviour, we referred to a previously identified core TF network linking IBD and CRC (Supplementary Figure S1).[21] Among the 24-core TFs and their regulated network in LSMCM-stimulated HT29 cells, two genes, *TGFBR2* and *TLR8*, were significantly upregulated (Table 1). Consistently, *TGFBR2* mRNA expression increased upon LSMCM addition (Supplementary Figure S3A). Furthermore, the application of anti-TGF*β*-neutralising antibodies prior to LMSCM significantly blunted EMT-related behavioural changes and migration/invasion in CRC cells (Figure 2b and c and Supplementary Figure S3B, S3C). Thus, TGF*β* signalling may be an important contributor to the observed changes in CRC cell behaviour.

Table 1 Differential expression of varied genes at the mRNA level in HT29 cell model

Gene	Fold change[a]	Gene	Fold change[a]
GFI1[b]	**−2.58**	BUB1B	1.32
TGFBR2	2.19	TLR8	2.19
TCF7L2	1.32	**RUNX3[b]**	**−1.14**
REG4	1.09	CD40	−1.24
HDAC5	1.15	CXCR4	−1.15
SMAD2	1.21	HDAC5	−1.09
MUC2	1.34	CXCL13	−1.32
PTGER2	4.80	CCR7	−1.17
TCF7L2[b]	**−1.00**	**SMAD2[b]**	**1.44**
RPS9	−1.02	**SOX10[b]**	**1.04**
APC	−1.12	**TFF3[b]**	**1.37**
PTPRH	−1.20	**SMAD7[b]**	**1.16**
ARHGEF4	−1.06	**ETS1[b]**	**1.12**
NAT1	−1.18	**POU5F1B[b]**	**−1.61**
STAT3[b]	**2.58**	**FOXO1[b]**	**−1.41**
AKT1	3.58	**HOXA4[b]**	**−1.30**
TP53I3	2.58	**NFYB[b]**	**−1.05**
XBP1[b]	**−1.60**	**FOXC1[b]**	**−1.20**
C5	−1.42	**ZNF589[b]**	**1.07**
CCL24	−1.06	**TCF4[b]**	**1.12**
CHST2	−1.20	**SREBF[b]**	**−1.13**
IL1B	−1.16	**CEBPG[b]**	**1.16**
PBX1[b]	**1.80**	**NFATC1[b]**	**−1.07**
IL23R	1.14	**PROM1[b]**	**1.05**
COX1	1.21	**BACH2[b]**	**−1.26**
TYMS	1.64	**POU2F2[b]**	**1.02**

[a]Cells were treated with LSMCM for 24 h. Gene expression showing at least twofold change was recognised in red as being significantly altered. Consistent results from independent real-time PCR assays were obtained. [b]Transcriptional factor, others are their related genes. The bold entries indicate the transcriptional factors

Inflammation-linked changes in CRC cell behaviour resulting from multiple factors in the cell model system. CRC cells exhibited maximal behavioural changes after treatment for 24 h with LSMCM. To investigate the factors driving these changes, we examined the expression of multiple effectors in HT29 cells for up to 96 h. The expressions of *GFI1* and *STAT3* were significantly altered upon LSMCM treatment, and the GFI1-associated factors *PTGER2* (coding for EP2), *TGFBR2*, and STAT3-associated *AKT1* were upregulated (Table 1). In addition, we examined ERK1/2, NF-*κ*B (p65 subunit), EMT-related Snail, Zeb1, and Twist in the expression analysis, considering their effects on inflammation and metastasis.[33,34] We observed sequential changes in the expression or activities of almost all of these effectors for up to 96 h at the protein level (Figure 2d and Supplementary Figure S3D). Two of the earliest changes were decreased GFI1 and increased ERK phosphorylation. Moreover, the expression of the GFI1-repressed gene *PTGER2* expectedly increased upon LSMCM addition (Figure 2e). Other changes subsequently occurred, including the activation of STAT3, EP2, AKT, and p65 (Figure 2d);

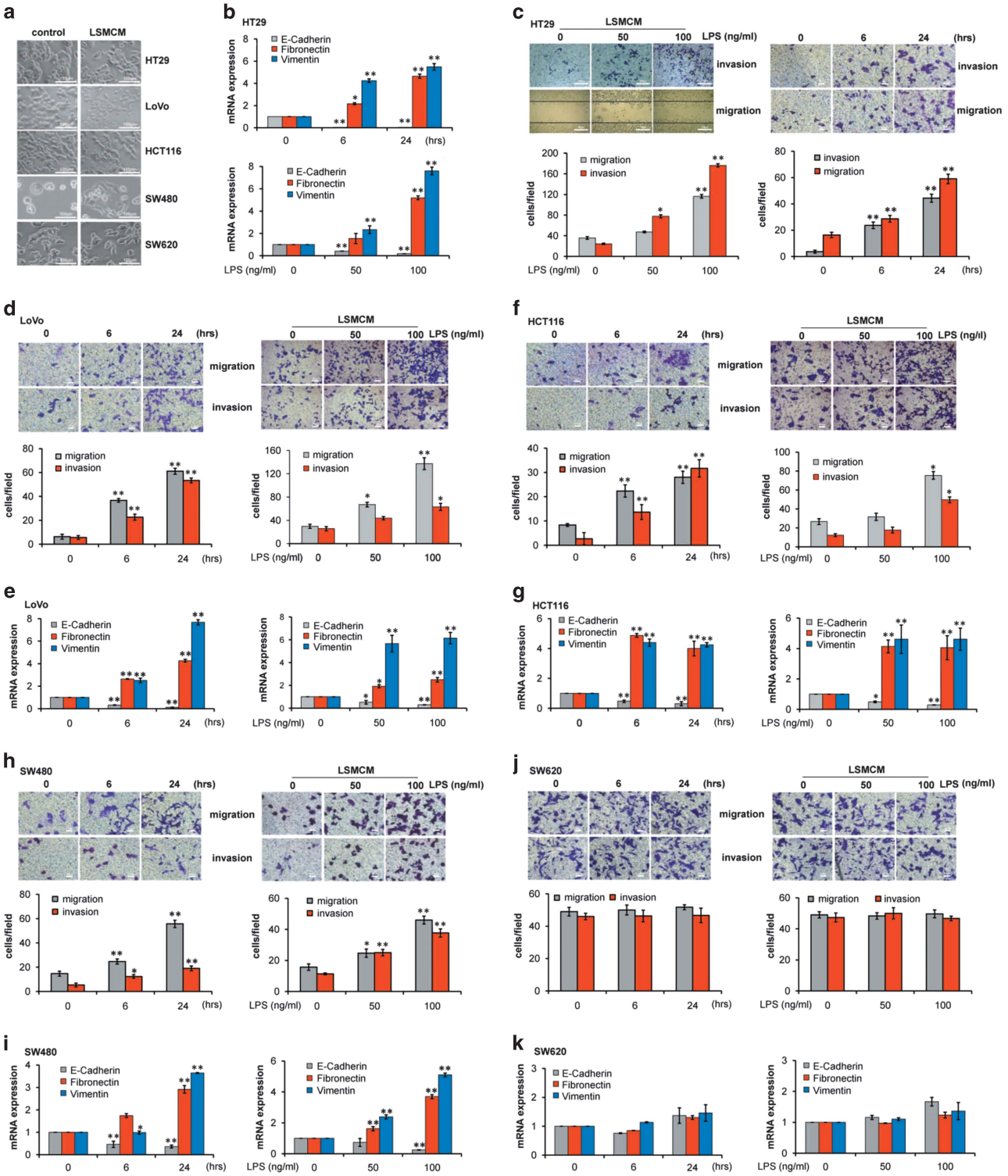

Figure 1 LSMCM increases CRC cell metastatic behaviour. (**a**) Culture with LSMCM induces morphology changes in HT29, LoVo, HCT116, SW480, and SW620 cells. (**b**) qRT-PCR of E-cadherin, Fibronectin, and Vimentin mRNA in HT29 with LSMCM for different times or prepared from supernatant of THP1 cells that were incubated with different LPS concentrations. (**c**) HT29 cells were treated with LSMCM for different times; or prepared from supernatant of THP1 cells that were incubated with different LPS concentrations. Cell migratory and invasive activities were measured and quantified. (**d**) LoVo cells were treated as in (**c**) and their migratory and invasive activity was measured and quantified. (**e**) qRT-PCR of E-cadherin, Fibronectin and Vimentin mRNA in LoVo cells treated as in (**b**). Results of similar experiments were exhibited for HCT116 cells, SW480 cells and SW620 cells, respectively, in (**f**–**k**). (**b**–**k**) show means ± S.D. of three independent experiments. Statistically significant differences are indicated. $^{*}P<0.05$; $^{**}P<0.01$

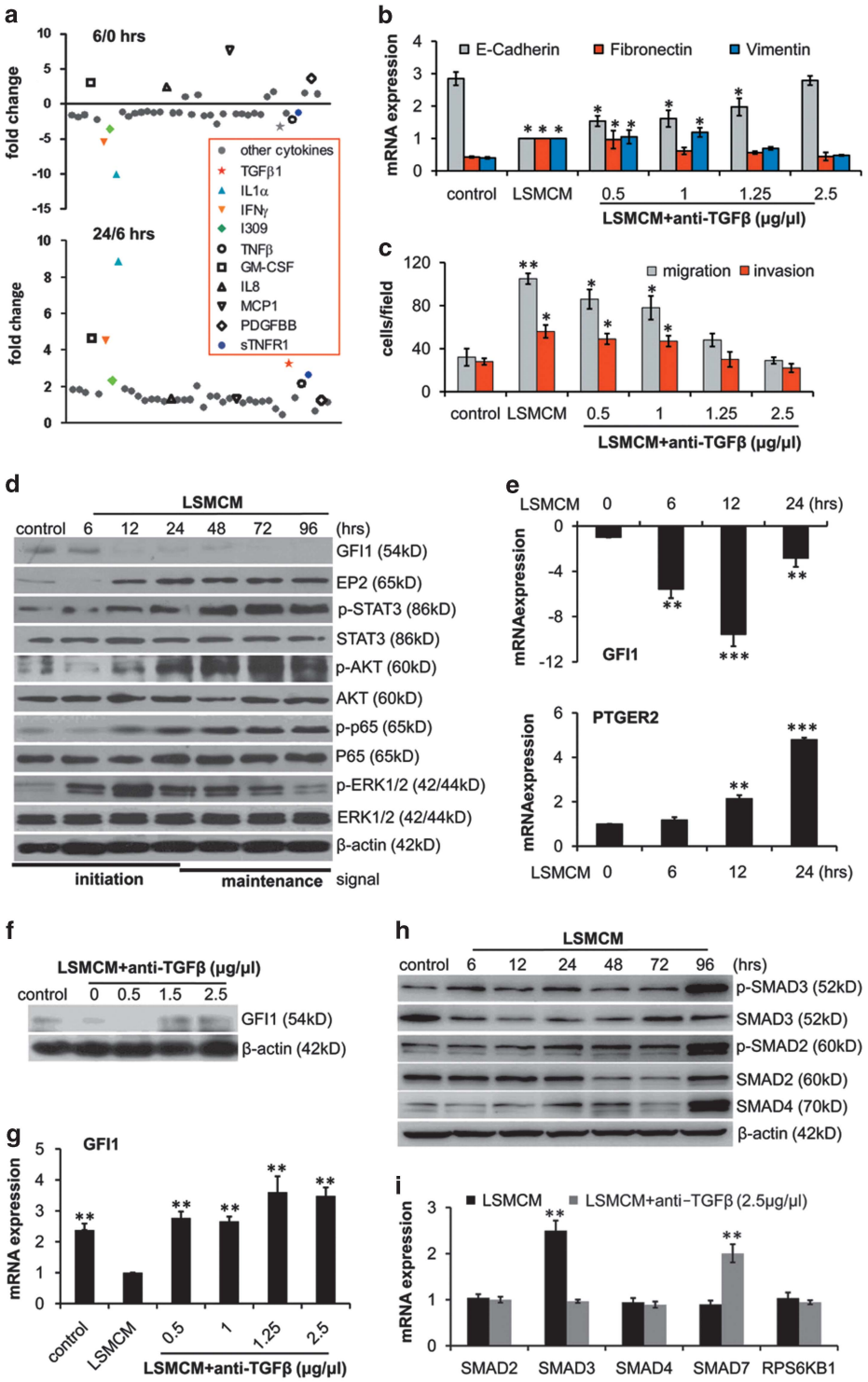

Figure 2 Monocyte-derived TGFβ downregulates GFI1 and induces EMT and cell metastatic behaviour. (**a**) Cytokines in culture medium from HT29 cells treated with LSMCM for 6 or 24 h were measured by Cytokine antibody arrays. Results shown are fold changes compared with freshly collected LSMCM. (**b**) qRT-PCR of E-cadherin, Fibronectin, and Vimentin mRNA in HT29 cells treated with LSMCM with/without anti-TGFβ-neutralising antibodies for 24 h. (**c**) Quantification of data shown in Supplementary Figure S3B, depicting the role of TGFβ in LSMCM-induced changes in cell behaviour. (**d**) HT29 cells were incubated with LSMCM for up to 96 h. Whole-cell lysates were prepared at the indicated time points and analysed for expression and phosphorylation of the indicated proteins. (**e**) Time course of GFI1 and PTGER2 mRNA expression in HT29 cells treated with LSMCM by qRT-PCR. (**f**) Effect of anti-TGFβ-neutralising antibodies on LSMCM-induced suppression of GFI1 expression. (**g**) qRT-PCR of GFI1 mRNA in HT29 cells treated with LSMCM plus indicated concentrations of anti-TGFβ-neutralising antibodies. (**h**) HT29 cells were treated with LSMCM for up to 96 h, and the expression or phosphorylation of SMAD2/3/4 were analysed. (**i**) qRT-PCR of SMAD2, SMAD3, SMAD4, SMAD7, and RPS6KB1 mRNA in HT29 cells treated with LSMCM or LSMCM plus 2.5 μg/μl anti-TGFβ neutralising antibodies. (**b**), (**c**), (**e**), (**g**), (**i**) show means $\pm$ S.D. of three independent experiments. Statistically significant differences are indicated. $^{*}P < 0.05$; $^{**}P < 0.01$; $^{***}P < 0.001$

increased expressions of Snail and Zeb1, but not Twist (Supplementary Figure S3D).

Significantly, the LSMCM-induced GFI1 decrease was reversed by TGFβ neutralisation in a dose-dependent manner in HT29 cells (Figure 2f and g). Further assays indicated that TGFβ might exert this effect via SMAD-dependent pathways. Notably, phospho-SMAD3 was significantly elevated as early as 6 h and remained activated for 96 h; phospho-SMAD2 and the expression of SMAD4 were also elevated (Figure 2h). Conversely, TGFβ neutralisation reversed the LSMCM-mediated SMAD3 elevation (Figure 2i). Notably, the expression of *RPS6KB1*, a factor in SMAD-independent pathways, was unaffected by either LSMCM or additional TGFβ neutralisation (Figure 2i). Furthermore, in the supernatant, three other cytokines, IL1α, TNFβ, and IFNγ, whose expression changes were similar to those of TGFβ under LSMCM treatment (Figure 2a), led to GFI1 downregulation and the activation of cellular downstream effectors to varied extents (Supplementary Figure S3E–G). Collectively, these results showed that effects of multiple factors contributed to the transformation of CRC cells under LSMCM treatment.

GFI1 is a gating regulator in the cellular transformation of CRC cells. We next examined whether decreased GFI1 expression affected the aforementioned changes in HT29 cells. Forced GFI1 expression decreased *PTGER2* (gene name for EP2) mRNA (Figure 3a) but not vice versa (Figure 3b), although a potential GFI1 binding site was detected in the *STAT3* promoter but not in *PTGER2* (Figure 3c). Chromatin immunoprecipitation (ChIP) assays confirmed less and less GFI1 bound to the endogenous *STAT3* promoter during LSMCM stimulation (Figure 3d). GFI1 expression significantly decreased phosphorylated and total STAT3 (Figure 3e). Luciferase reporter assays revealed specific binding between GFI1 and the indicated sequence (Figure 3c) in the *STAT3* promoter (Figure 3f). Furthermore, *STAT3* siRNA treatment moderately reduced EP2 protein expression (Figure 3g) but not its mRNA expression (Supplementary Figure S4A). Conversely, *PTGER2* siRNA treatment did not affect STAT3 expression or activation by LSMCM (Figure 3h, Supplementary Figure S4B). We subsequently detected the physical interaction between STAT3 and EP2, which was further enhanced after LSMCM treatment (Figure 3i, Supplementary Figure S4C), but not transcriptional regulation of STAT3 on *PTGER2* (Supplementary Figure S4D). Thus, the GFI1-STAT3-EP2 signalling cascade is activated in HT29 cells under LSMCM stimulation.

Moreover, although GFI1-expressing cells showed decreased ERK1/2 phosphorylation (Figure 3j), ERK1/2 siRNA, or U0126 (an MEK inhibitor) treatment reduced EP2 expression at the protein level (Figure 3k, Supplementary Figure S4E) but not mRNA (Supplementary Figure S4F). However, *PTGER2* siRNA had no effect on ERK1/2 phosphorylation (Figure 3l). In addition, we observed physical interactions between ERK1/2 and EP2 (Figure 3m). These data suggest that, similar to STAT3, ERK1/2 activation upon GFI1 reduction contributed to increased EP2 expression. In response to LSMCM treatment, the activation of AKT and p65 was observed later than EP2 upregulation (Figure 2d). *PTGER2* siRNA treatment reduced both AKT and p65 phosphorylation (Figure 3n). Furthermore, the inhibition of AKT phosphorylation using Ly294002 reduced p65 phosphorylation; *RELA* (coding for p65) siRNA, or PDTC (an inhibitor of NF-κB activation) had only a minor effect on AKT phosphorylation (Figure 3o, Supplementary Figure S4G). These data suggest the existence of an EP2-AKT-NF-κB cascade.

GFI1 downregulation enhances the metastasis of human CRC cells. To determine whether the activation of signalling effectors affects the consequent production of cytokines, we examined expressions of 10 cytokines in HT29 cells incubated in LSMCM for 24 h. The results showed that, except for IFNγ (data not shown), the mRNA expression of GM-CSF, IL8, MCP1, PDGFBB, sTNFR1, TGFβ1, IL1α, I309, and TNFβ significantly increased (Figure 4a). Moreover, ELISA showed a significant decrease in TGFβ production at 6 h and a return to basal amounts at 24 h after LMSCM addition (Figure 4b), consistent with previous data (Figure 2a). We next applied shRNA, siRNA or gene overexpression to *GFI1*, *PTGER2*, *STAT3*, or *RELA* in the cell model. The results showed that forced GFI1 expression suppressed all 9 cytokines at the mRNA level, but GFI1 knockdown induced the expression of these molecules; *PTGER2* siRNA had only moderate inhibition effects. In comparison, gene knockdown of *STAT3* or *RELA* had variable effects, inhibiting the expression of certain cytokines while increasing others (Figure 4c). Collectively, the most consistent effect of LSMCM incubation was the repression of GFI1, which acts as a suppressor of cytokine gene expression. The effect of decreased GFI1 may be mediated via STAT3 and ERK1/2, which stimulate EP2 expression (Figure 4d).

Moreover, *GFI1* overexpression in LMSCM-stimulated HT29 cells reversed the changes in the expression of EMT markers and greatly inhibited cell migration and invasion (Figure 4e and f); conversely, *GFI1* knockdown significantly enhanced cell migration & invasion, induced EMT (Figure 4g and h), and increased EP2 expression and STAT3, p65, AKT, and ERK phosphorylation (Supplementary Figure S4H). Keeping consistent, we further showed that although SW480 cells exhibited the weakest response and SW620 cells exhibited the strongest response to LSMCM stimulation, the expression of GFI1 was the highest in SW480 cells and lowest in SW620 cells among the tested CRC cells (Figure 5a and b). In parallel, forced GFI1 expression in SW620 cells significantly reduced cell migration and invasion and vice versa (Figure 5c–f). Whereas SW620 cells poorly responded to LSMCM stimulation (Figure 1a, j and k), forced GFI1 expression greatly enhanced SW620 sensitivity to LSMCM (Figure 5g). Collectively, these data indicated an essential role for GFI1 downregulation in coordinating the changes in the cell behaviour and metastatic potential of CRC cells.

GFI1/Gfi1 inhibits CRC metastasis to distal sites. We further examined GFI1 effect *in vivo*. GFI1 overexpression and control HT29 cells incubated with LMSCM for 24 h were subcutaneously (s.c.) transplanted into DKO (BALB/c-*Rag2*$^{-/-}$*gc*$^{-/-}$) mice, and the s.c. tumour masses were harvested. The tumour growth rates, volume and mouse body weight were similar between the two groups of animals

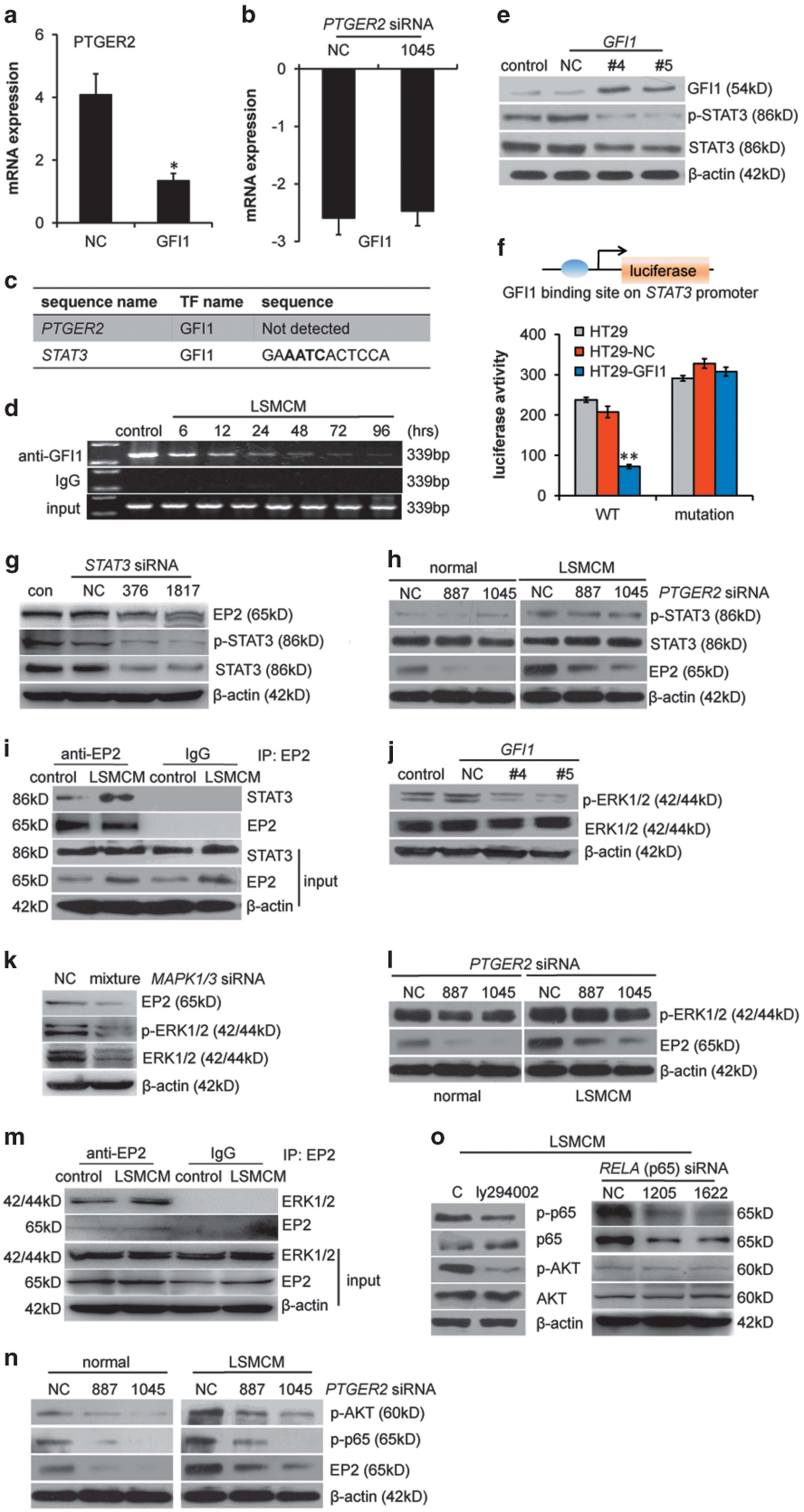
a
PTGER2
mRNA expression
NC
GFI1
b
PTGER2 siRNA
NC
1045
mRNA expression
GFI1
c
sequence name | TF name | sequence
PTGER2 | GFI1 | Not detected
STAT3 | GFI1 | GAAATCACTCCA
d
LSMCM
control 6 12 24 48 72 96 (hrs)
anti-GFI1
IgG
input
339bp
e
GFI1
control NC #4 #5
GFI1 (54kD)
p-STAT3 (86kD)
STAT3 (86kD)
β-actin (42kD)
f
luciferase
GFI1 binding site on STAT3 promoter
HT29
HT29-NC
HT29-GFI1
luciferase avtivity
WT
mutation
g
STAT3 siRNA
con NC 376 1817
EP2 (65kD)
p-STAT3 (86kD)
STAT3 (86kD)
β-actin (42kD)
h
normal
LSMCM
NC 887 1045 NC 887 1045 PTGER2 siRNA
p-STAT3 (86kD)
STAT3 (86kD)
EP2 (65kD)
β-actin (42kD)
i
anti-EP2
IgG
IP: EP2
control LSMCM control LSMCM
86kD STAT3
65kD EP2
86kD STAT3
65kD EP2
42kD β-actin
input
j
GFI1
control NC #4 #5
p-ERK1/2 (42/44kD)
ERK1/2 (42/44kD)
β-actin (42kD)
k
NC mixture MAPK1/3 siRNA
EP2 (65kD)
p-ERK1/2 (42/44kD)
ERK1/2 (42/44kD)
β-actin (42kD)
l
PTGER2 siRNA
NC 887 1045 NC 887 1045
p-ERK1/2 (42/44kD)
EP2 (65kD)
β-actin (42kD)
normal
LSMCM
m
anti-EP2
IgG
IP: EP2
control LSMCM control LSMCM
42/44kD ERK1/2
65kD EP2
42/44kD ERK1/2
65kD EP2
42kD β-actin
input
o
LSMCM
RELA (p65) siRNA
C ly294002
NC 1205 1622
p-p65
p65
p-AKT
AKT
β-actin
65kD
65kD
60kD
60kD
42kD
n
normal
LSMCM
NC 887 1045 NC 887 1045 PTGER2 siRNA
p-AKT (60kD)
p-p65 (65kD)
EP2 (65kD)
β-actin (42kD)

before and after tumour cell transplantation (Supplementary Figure S5A-E). Immunoblot analysis confirmed GFI1 overexpression and the decreased expression of STAT3, Snail, and Zeb1 in GFI1-positive tumours *in vivo* (Supplementary Figure S5F).

Next, we injected cultured GFI1-expressing (GFI1-T) and NC-T s.c. tumour cells via the tail vein (t.v.) into DKO mice (Supplementary Figure S5G). LSMCM stimulation for 24 h prior to tumour cell injection greatly accelerated lung metastasis in the NC-T group, reducing latency from 90 to 30 d compared with cells not subjected to LSMCM stimulation (data not shown). Moreover, significantly more lung metastases were observed in the NC-T than GFI1-T group at 30 d (Supplementary Figure S5H, I). Furthermore, at 60 d, all eight NC-T mice and only one of the eight GFI1-T mice showed lung metastases, whereas three out of eight NC-T and no GFI1-T mice showed secondary metastasis to the liver, with significantly larger metastases in the lungs of NC-T mice (Supplementary Figure S6A-F). In addition, NC-T mice exhibited more weight loss compared with GFI1-T mice (Supplementary Figure S6G). H&E staining of the lung biopsies showed that the NC-T mice had more macroscopic tumours than GFI1-T mice; and NC-T liver metastases were also large (Supplementary Figure S6B, E).

To further investigate the role of murine Gfi1 in CRC cell metastasis in immune competent mice, we constructed MC38-Gfi1 and MC38-con cell lines using CRISPR/Cas9 technology. Forced *Gfi1* activation in metastatic MC38 CRC cells reduced the rates of cell migration and invasion, diminished the expressions of EP2 and STAT3, and attenuated STAT3, AKT, and p65 phosphorylation (Figure 6a and b). We next intrasplenically (i.s.) injected these cells into syngeneic C57BL/6 mice and subsequently examined liver metastases and disease progression. Gfi1 overexpression greatly reduced tumour metastatic incidence (Supplementary Figure S6H), liver metastases sizes and body weight in age-matched groups (Figure 6c–f). In addition, MC38-Gfi1 mice survived much longer than the control mice (Figure 6g).

GFI1 downregulation increased the metastatic ability of CRC cells *in vivo*. HT29 cells harbouring *GFI1* gene knockdown by shRNA or control plasmid were s.c. transplanted into nude mice and harvested at 20 d. The results showed no significant differences between the two groups of mice in animal body weight, tumour formation rate, and tumour weight and volume (Supplementary Figure S7A–E), although shGFI1 tumours seemed smaller than the controls (Supplementary Figure S7C, D). Next, we injected these two groups of cells via the t.v. into the mice. At 40 d after injection, all of the lungs from the shGFI1 mice and none of the lungs from control mice developed pronounced lung metastases (Supplementary Figure S7F, G). *GFI1* knockdown had a minor effect on the body weight of the mice; H&E staining revealed that the lungs from shGFI1 mice showed aggregated CRC cells around the blood vessels to form larger metastases (Supplementary Figure S7H, I).

To determine whether GFI1 downregulation correlated with CRC metastatic progression in humans, we analysed a TCGA data set including 155 patient biopsies from primary tumour sites. The results indicated that the primary tumours from patients with metastatic CRC (M1) expressed significantly less GFI1 than those from patients who did not progress to metastatic disease (M0) (Figure 6h). Collectively, these data strongly suggest that GFI1 downregulation promotes CRC metastasis to distant organs.

Loss of GFI1 in advanced human CRC samples. To further relate GFI1 expression with CRC metastasis, we examined a series of human biopsies, including normal colon tissues ($n=10$), cancer adjacent normal colonic tissue ($n=10$), precancerous colon lesions ($n=5$ adenomatous and $n=5$ polyp tissues), CRC ($n=23$) and CRC metastatic lesions ($n=23$) using IHC (Figure 7a). The loss of GFI1 expression was primarily observed in advanced CRC (stage IIB and higher) and metastases compared with normal and lower stage tissues, respectively (Figure 7b and c). Decreased GFI1 expression was initially observed at stage IIB and further decreased at stage III (Figure 7a), suggesting that GFI1 dowregulation likely precedes metastatic spread. In addition, in the same set of human samples, the markedly increased expression of STAT3 was observed in CRC compared with normal biopsies (Supplementary Figure S8A, B), although the expression was similar between early- and late-stage tumour samples (Supplementary Figure S8C). Moreover, a negative correlation between GFI1 and STAT3 expression at the protein level was observed across all categorised sample sets, and significantly correlated expression was only observed in normal colon specimens and metastases (Supplementary Figure S8D). These data

Figure 3 GFI1 is a gating regulator that controls CRC cell metastatic activity. (**a**) qRT-PCR of PTGER2 mRNA in HT29 cells transfected with GFI1-encoding or control plasmid. (**b**) qRT-PCR of GFI1 mRNA in HT29 cells treated with PTGER2 siRNA or NC. (**c**) Analysis of GFI1 binding sites in *PTGER2* or *STAT3* promoters. (**d**) ChIP assays of GFI1 recruitment to the *STAT3* promoter in HT29 cells incubated with LSMCM for up to 96 h. The data are presented as enrichment of precipitated DNA from chromatin incubated with an anti-GFI1 antibody versus IgG. (**e**) GFI1 and STAT3 expression and phosphorylation in HT29 cell transfected with control or GFI1-encoding plasmids. (**f**) Luciferase assays measuring GFI1 -repressive activity in HT29 cells transfected with *STAT3* promoter (WT) or (mutant)-luc plasmid. (**g**) EP2 and STAT3 protein expression and phosphorylation in HT29 cells treated with control or *STAT3* siRNA. (**h**) STAT3 expression and phosphorylation in HT29 cells treated with *PTGER2* or control siRNA. (**i**) Co-IP assays of STAT3 binding to EP2 in HT29 cells treated with or without LSMCM. Data are presented as enrichment of precipitated protein from whole-cell lysates immunoprecipitation with an anti-EP2 antibody or non-specific IgG. (**j**) Total and phosphorylated ERK1/2 levels in HT29 cells transfected with the GFI1-encoding plasmid or control. (**k**) EP2, ERK1/2, and phosphor-ERK1/2 expression in HT29 cells pretreated with *MAPK1/3* siRNA or control. (**l**) ERK1/2 phosphorylation in HT29 cells treated with *PTGER2* siRNA or control. (**m**) Co-IP assays of ERK1/2 binding to EP2 in HT29 cells treated with or without LSMCM. (**n**) AKT and p65 phosphorylation in HT29 cells transfected with control (NC) or *PTGER2* siRNA with or without LSMCM. **(o)** AKT and p65 phosphorylation in HT29 cells pretreated with or without 20 μM PI3K inhibitor (Ly294002) or *RELA* siRNA for 12 h, followed by treatment with LSMCM or LSMCM plus respective inhibitors or siRNA for 24 h. Results in (**a**), (**b**), and (**f**) are shown as means $\pm$ S.D. of three independent experiments. Statistically significant differences are indicated. $^{*}P<0.05$; $^{**}P<0.01$

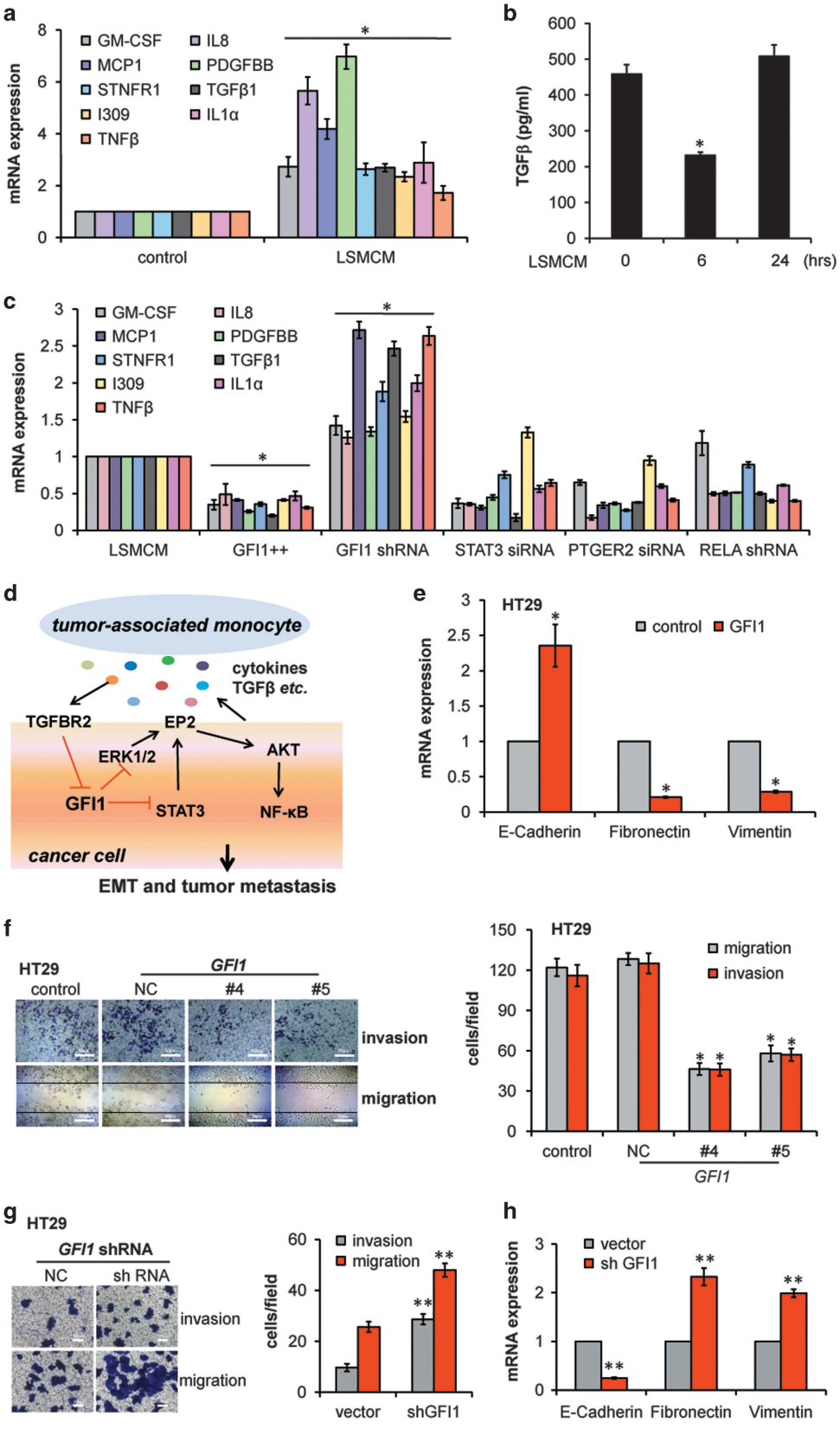
a
mRNA expression
GM-CSF
MCP1
STNFR1
I309
TNFβ
IL8
PDGFBB
TGFβ1
IL1α
control
LSMCM
b
TGFβ (pg/ml)
LSMCM
0
6
24
(hrs)
c
mRNA expression
LSMCM
GFI1++
GFI1 shRNA
STAT3 siRNA
PTGER2 siRNA
RELA shRNA
d
tumor-associated monocyte
cytokines
TGFβ etc.
TGFBR2
EP2
ERK1/2
AKT
GFI1
STAT3
NF-κB
cancer cell
EMT and tumor metastasis
e
HT29
control
GFI1
mRNA expression
E-Cadherin
Fibronectin
Vimentin
f
HT29
GFI1
control
NC
#4
#5
invasion
migration
HT29
migration
invasion
cells/field
control
NC
#4
#5
GFI1
g
HT29
GFI1 shRNA
NC
sh RNA
invasion
migration
invasion
migration
cells/field
vector
shGFI1
h
vector
sh GFI1
mRNA expression
E-Cadherin
Fibronectin
Vimentin

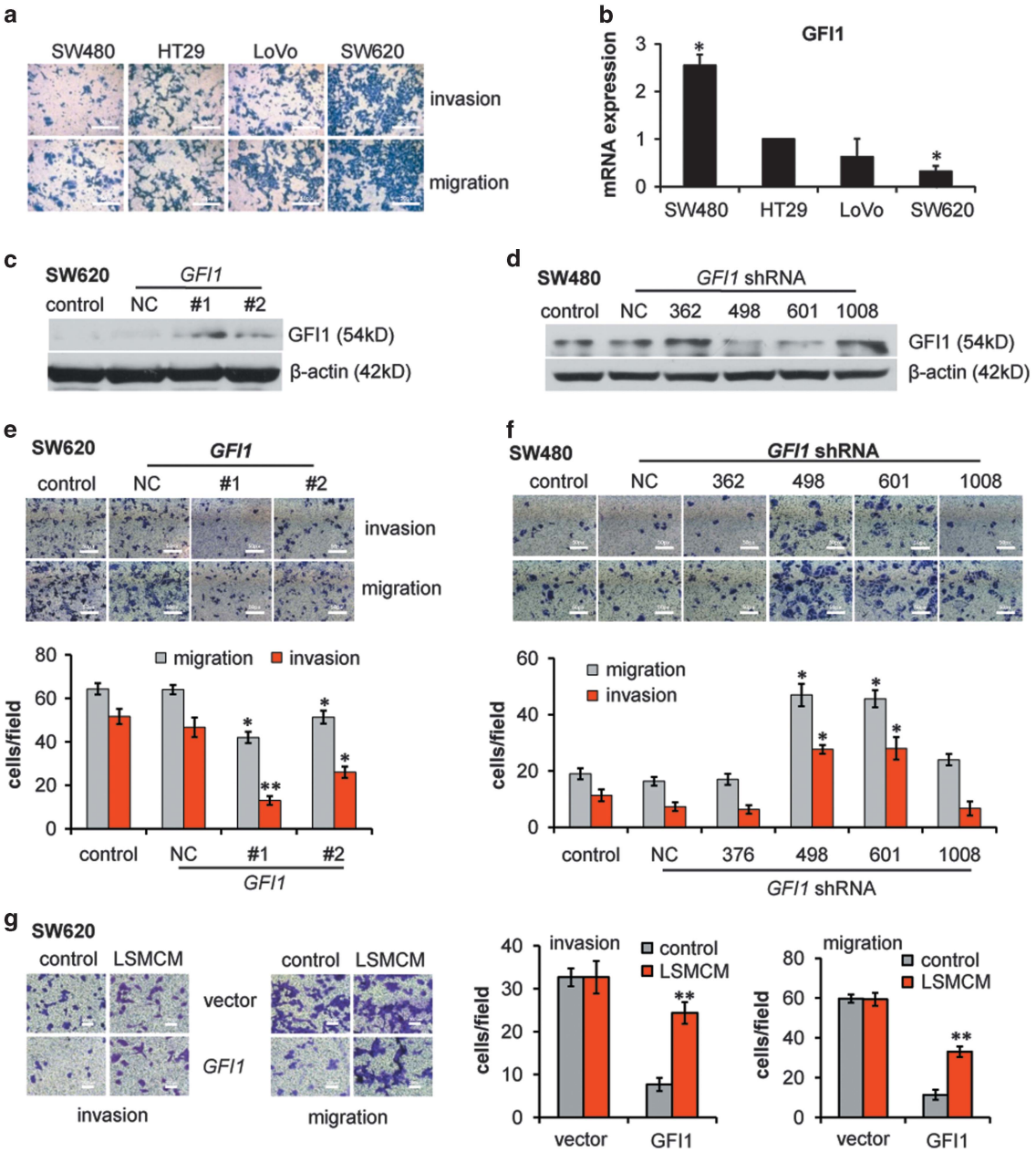

Figure 5 GFI1 controls invasive and metastatic behaviour of CRC cells. (**a**) Invasive and migratory activity of different CRC cell lines (SW480, HT29, LoVo, SW620). (**b**) qRT-PCR of GFI1 mRNA in three other human CRC cells shown relative to GFI1 mRNA content of HT29 cells. (**c**) GFI1 protein expression in SW620 cells transfected with GFI1-encoding plasmid or control. (**d**) GFI1 protein expression in SW480 cells transfected with GFI1 shRNA plasmid or control. (**e**) Migratory and invasive behaviour of SW620 cells transfected with negative control or GFI1-encoding plasmids or control. (**f**) Migratory and invasive behaviour of SW480 cells transfected with negative control or GFI1 shRNA plasmids or control. (**g**) Migratory and invasive behaviour of SW620 cells transfected with negative control or GFI1-encoding plasmids upon LSMCM stimuli. (**b**), (**e**–**g**) are shown as means ± S.D. of three independent experiments. Statistically significant differences are indicated. $^{*}P<0.05$; $^{**}P<0.01$

Figure 4 GFI1 controls an inflammatory signalling circuit that enhances invasive and migratory behaviour of human CRC Cells. (**a**) qRT-PCR of indicated cytokine mRNA in HT29 cells incubated with control medium or LSMCM for 24 h. (**b**) TGFβ concentrations by ELISA assays in supernatants from HT29 cells that were treated with LSMCM for the indicated periods. (**c**) qRT-PCR of shown cytokine mRNA in HT29 cells treated with LSMCM or LSMCM with the indicated shRNAs, siRNAs, or GFI1-expressing plasmids. (**d**) Schematic overview of the inflammation and TGFβ-induced regulatory circuit that controls CRC cell metastatic behaviour. (**e**) qRT-PCR of E-cadherin, Fibronectin, and Vimentin mRNA in HT29 cells transfected with GFI1-encoding plasmid or control. (**f**) Regulation of HT29 invasive and migratory behaviour by ectopically expressed GFI1. (**g**) Regulation of HT29 invasive and migratory behaviour by knocking down of GFI1 expression. (**h**) qRT-PCR of E-cadherin, Fibronectin and Vimentin mRNA in HT29 cells transfected with GFI1 shRNA or control. (**a**–**c**), (**e**–**h**) are shown as means ± S.D. of three independent experiments. Statistically significant differences are indicated. $^{*}P<0.05$; $^{**}P<0.01$

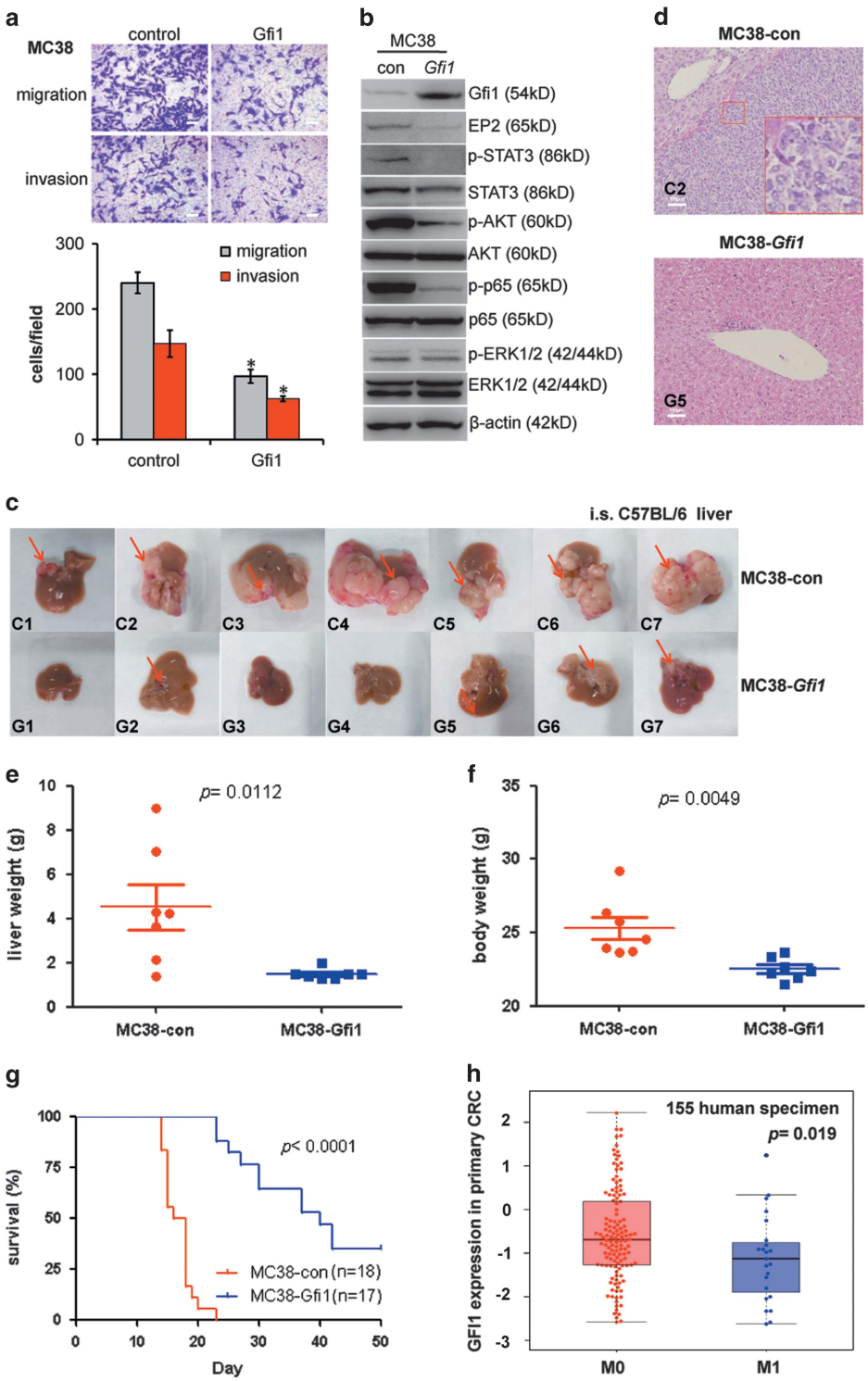

Figure 6 Gfi1 inhibits MC38 metastasis to liver. (**a**) Migratory and invasive activity of MC38 cells transfected with control or Gfi1-activation plasmids. (**b**) Immunoblot analysis of MC38-con and MC38-Gfi1 cells demonstrating effects of Gfi1 on indicated signalling proteins. (**c**) Liver metastases in mice injected intrasplenicly (i.s.) with MC38-con or MC38-Gfi1 cells. Arrows pointed to metastases in the liver. (**d**) Representative H&E-stained sections of the livers of mice injected with MC38-Gfi1 or MC38-con cells. (**e**) Weights of livers in mice injected with MC38-Gfi1 or MC38-con cells 16 days after i.s. injection. (**f**) Weight of mice injected with MC38-Gfi1 or MC38-con cells 16 days after i.s. injection. (**g**) Kaplan–Meier survival curve in respective MC38-Gfi1 and -con mice, log-rank test, $P<0.0001$. (**h**) GFI1 expression levels in the primary tumour of human CRC in patients who did (M1) or did not (M0) develop distal metastases in a TCGA data set

suggest that GFI1 downregulation may be highly correlated with increased STAT3 expression in CRC human samples.

To confirm the role of GFI1 in an even larger number of clinical samples, we examined the public databases of colon cancer data sets, including CRC data from TCGA, GSE17538, GSE41258, and GSE14333, comprising a total of 918 clinical samples. Notably, a significant decrease in GFI1 expression was observed in advanced CRC relative to early-stage tumours (Figure 7d). To evaluate the clinical prognosis value of GFI1 expression, we used another set of CRC data containing 177 samples harbouring relapse-free survival time (GSE39582). By stratifying cancer patients according to GFI1 mRNA expression (median), we observed that lower GFI1 mRNA expression was associated with decreased patient survival (Figure 7e). Interestingly, a significant GFI1 loss was also observed in adenomas and polyps compared with normal tissues (Figure 7f), suggesting that this loss might be an early event in colon carcinogenesis that needs to exceed a certain threshold to enable cancer cells to acquire metastatic properties.

Discussion

Cancer metastasis is a multi-step process relying on tumour–stroma interactions. Inflammation greatly contributes to CRC development and progression.[20,35,36] In the present study, we identified an inflammatory environment-mediated transcriptional programme that controls the metastatic potential of CRC through GFI1, a transcriptional repressor. Curiously, a key cytokine responsible for GFI1 downregulation is TGFβ. Although in early CRC cells and premalignant lesions, the TGFβ signalling pathway has tumour-suppressive activities,[37–39] the pro-metastatic activity of this signalling pathway is observed in more advanced cancer.[40,41] These results suggest that tumour stromal cytokines may accomplish pro-metastatic activity through GFI1. Importantly, the analysis of human clinical specimens confirmed that GFI1 downregulation correlated with increased CRC metastasis.

Previously, GFI1 demonstrated importance in the lineage decision process during IEC differentiation,[30,31] but the results of the present study are the first to implicate GFI1 as a negative regulator of CRC metastasis. GFI1 downregulation during the metastatic progression of CRC may reflect increased TGFβ1 expression in TGFβR- and SMAD2/3-expressing CRC cells.[42] In addition, using a cell model of inflammation-driven metastasis, we verified that other cytokines, such as IL1α, TNFβ or IFNγ in the tumour microenvironment also contributed to GFI1 decrease, thereby activating CRC cell metastatic behaviours; yet the effect of the cytokine combination or other factors needs further verification. Consistently, some of these cytokines, or conditioned medium from TAMs, were implicated in EMT-like processes and promoting metastatic behaviours in CRC cells.[43–47] Moreover, NF-κB and/or STAT3 signalling and the feed-forward activation circuit in CRC cells may support metastasis to remote organs.[48–50]

STAT3 has been demonstrated as an important player in inflammation-associated CRC progression.[15,51,52] Our data highlight STAT3 as a core TF in the inflammation-mediated TF network that controls CRC metastasis and showed that GFI1 expression inhibits STAT3 activation. Previous studies showed that GFI1 enhanced STAT3 activation through interactions with the STAT3 inhibitor PIAS3.[29] In contrast, the results of the present study showed that although GFI1 controlled STAT3 transcription through binding to its promoter, GFI1 downregulation triggered via LMSCM abrogated the effect, resulting in STAT3 activation. This variation suggests the operation of a context-dependent regulatory circuit. Consistent with other data,[41,53–55] we verified that EP2 signalling activation was highly relevant to inflammation-associated CRC progression.

It has been suggested that disseminated cancer cells are selected via stroma–tumour interactions before adapting to new microenvironmental conditions and giving rise to a metastatic clone.[38,56] There is a debate as to whether this selection occurs within or outside the primary tumour.[57] We observed that once GFI1 downregulation within CRC cells reaches a certain threshold, CRC cells become competent for metastatic spread as a result of the long-term activation of a regulatory circuit that is normally repressed by GFI1. The ectopic overexpression of GFI1/Gfi1 impaired the function of this signalling circuit and inhibited the metastatic activity of CRC cells, and vice versa. Although we observed that GFI1 expression is lost in human metastatic CRC and confirmed the ability of GFI1 to suppress metastatic spread, the CRC metastasis process is complex and likely to involve additional regulation.[20,58] For example, despite a strongly reverse relationship between GFI1 and STAT3 expression in normal human colorectal tissue samples, such a relationship was less pronounced in CRC samples (Supplementary Fig S8D and data not shown). As a gating regulator of CRC metastasis, GFI1 downregulation may elicit further feedback and/or network regulations on its downstream effectors, such as STAT3, besides other layers of disease complexity (Supplementary Figure S6I). Thus far, the dynamics of cellular adaptation resulting from genetic/epigenetic changes or phenotypic plasticity remain poorly understood in patients with advanced cancer.[59]

In summary, these findings elucidate a new mechanism contributing to the acquisition of metastatic potential during CRC progression. Therapeutic interventions that restore GFI1 expression may be suitable for the treatment of metastatic CRC, a condition that conveys high rates of mortality.

Materials and Methods

Cell culture, transfection, and treatment. THP1, U-937, HT29, LoVo, SW480, and SW620 cells from ATCC and MC38 cells granted from Dr. Shoshana Yakar were cultured at 37 °C and 5% CO_2 in Dulbecco's modified Eagle's medium or RPMI 1640 medium (Hyclone, Foster City, CA, USA) supplemented with 10% fetal bovine serum (FBS). Human cells were transfected using lipofectamine (Invitrogen, Grand Island, NY, USA). LSMCM were prepared from the supernatants of human THP1 cells mock stimulated or stimulated with Salmonella enteritidis-derived LPS (Sigma-Aldrich, St Louis, MO, USA) for 6 h. THP1 cells subsequently were centrifuged, and the supernatant was filtrated to eliminate any remaining cells. PBMC were isolated from human blood using lymphocyte separation solution, and then were induced into macrophage via IL4 and IL10 stimulation. U-937 cells also pretreated as PBMC. LSMφM were prepared like LSMCM using macrophages derived from PBMC or U-937 cells. CRC cells then were cultivated in the presence of regular medium or half LSMCM or LSMφM and half regular medium. Where indicated, cells were treated with anti-TGFβ neutralising antibody (Raybiotech, Norcross, GA, USA), 10 μM of U0126, 20 μM of Ly294002 or 10 μM of PDTC (Sigma-Aldrich) for the indicated times.

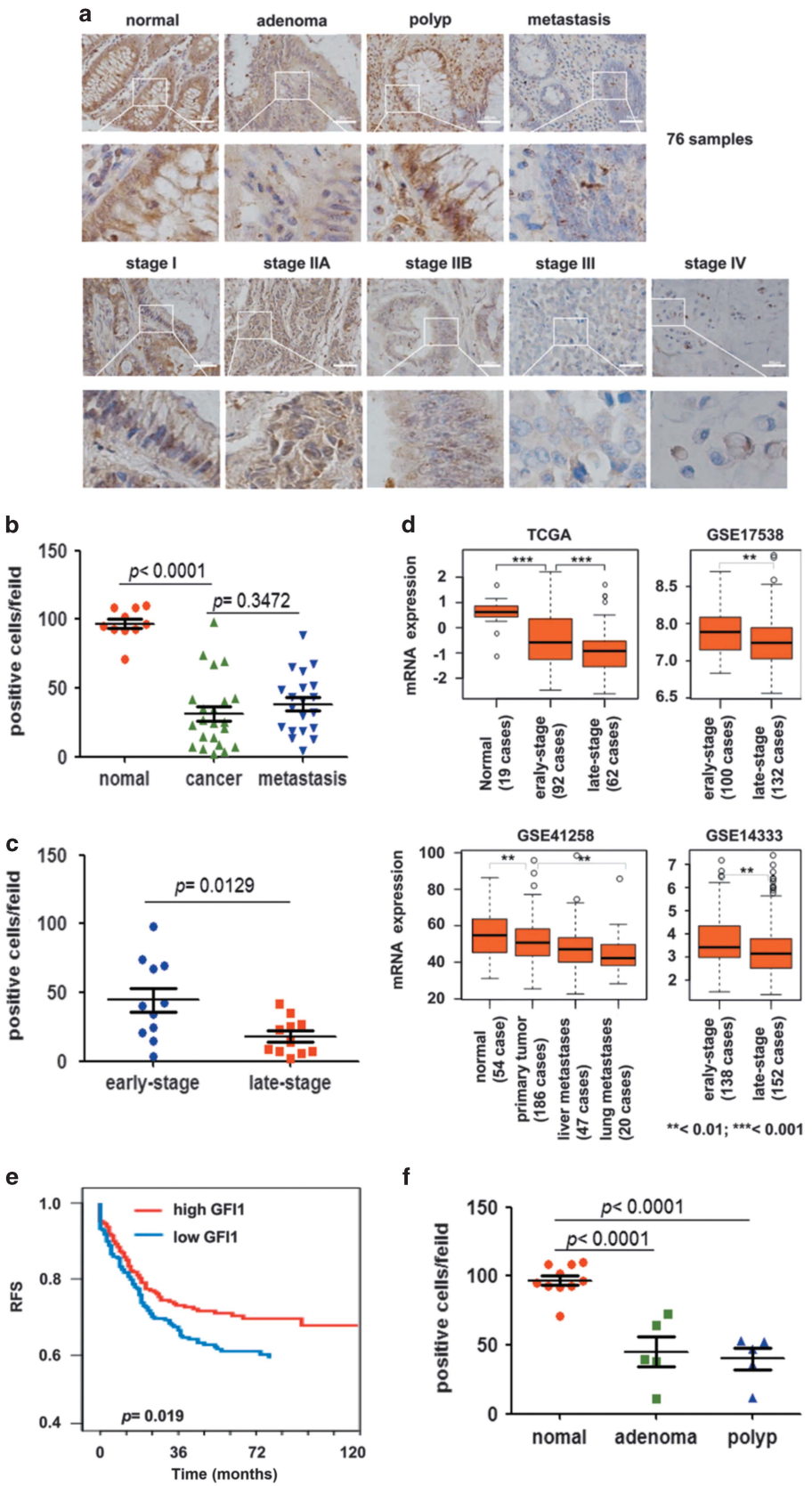
a
normal
adenoma
polyp
metastasis
76 samples
stage I
stage IIA
stage IIB
stage III
stage IV
b
positive cells/feild
p< 0.0001
p= 0.3472
nomal
cancer
metastasis
c
positive cells/feild
p= 0.0129
early-stage
late-stage
d
TCGA
GSE17538
mRNA expression
Normal (19 cases)
eraly-stage (92 cases)
late-stage (62 cases)
eraly-stage (100 cases)
late-stage (132 cases)
GSE41258
GSE14333
normal (54 case)
primary tumor (186 cases)
liver metastases (47 cases)
lung metastases (20 cases)
eraly-stage (138 cases)
late-stage (152 cases)
< 0.01; *< 0.001
e
RFS
high GFI1
low GFI1
p= 0.019
Time (months)
f
positive cells/feild
p< 0.0001
p< 0.0001
nomal
adenoma
polyp

Figure 7 Loss of GFI1 in Advanced Human CRC Samples. (**a**) Immunohistochemical analysis of GFI1 expression in normal, cancer, metastatic nodules, adenoma, and polyp colon tissues in a total of 76 human samples. (**b**) Number of GFI1 expression positive cells in human normal, CRC, and metastatic tissues (four sections evaluated per sample). (**c**) Number of GFI1 expression positive cells in human early-stage (I and II) CRC and late-stage (III and IV) CRC (four sections evaluated per sample). (**d**) GFI1 expression levels in normal colon and different tumour stages from TCGA, GSE17538, GSE41258, and GSE14333 data sets. (**e**) Relapse-free survival of CRC patients with relatively high and low GFI1 mRNA expression. (**f**) Number of GFI1-expressing cells in human normal, and pre-cancer tissues including adenoma, and polyp tissues (four sections evaluated per sample)

Construction of MC38-Gfi1 cells with CRISPR activation plasmids. To generate MC38-Gfi1 and -con cells, we used CRISPR Gfi1-activation plasmid (sc-437272) and control CRISPR/Cas9 plasmid (sc-418922, Santa Cruz Ltd., Dallas, CA, USA). Gfi1 CRISPR Activation Plasmid is a synergistic activation mediator transcription activation system designed to specifically upregulate gene expression according to manufacturer's instructions (Santa Cruz Ltd.). In brief, we infected MC38 cells with three plasmids at a 1:1:1 mass ratio: a plasmid encoding the deactivated Cas9 (dCas9) nuclease (D10A and N863A) fused to the transactivation domain VP64, and a blasticidin-resistant gene; a plasmid encoding the MS2-p65-HSF1 fusion protein, and a hygromycin-resistant gene; a plasmid encoding a target-specific 20 nt guide RNA (gRNA), and a puromycin-resistant gene. The positive cells were selected and cultured. Similar procedures were applied to generate MC38-con cells using control CRISPR activation plasmid.

Real-time PCR analysis. Total RNA was extracted using TRIzol (invitrogen). RNA was reverse transcribed using a Reverse Transcription kit (Applied Biosystems, Foster city, CA, USA). Real-time PCR was performed using SYBR green (Roche, Mannheim, Germany) on a Step One Real-time PCR System (Applied Biosystems). Expression data were normalised to GAPDH mRNA expression. Data were calculated as $2^{-\Delta\Delta Ct}$. Primer sequences are listed in Supplementary information.

ELISA and human antibody cytokine arrays. Culture medium was collected and subjected to ELISA analysis. Human TGFβ1 and TGFβ2 concentration were measured by ELISA (Raybiotech) according to the manufacturer's protocols. Measurement and analysis of Antibody Cytokine Arrays for 40 kinds of cytokines associated with macrophage were provided by Raybiotech.

Luciferase reporter assays. The pGL3-STAT3 or pGL3-STAT3-mut (BOSHI Ltd., Harbin, China) was transfected into HT29, HT29-NC, and HT29-GFI1 cells using lipofectamine 2000 (Invitrogen). Luciferase activity was measured 48 h after transfection.

Migration and invasion assays. About 4000 cells were seeded into the upper chambers in 100 μl of the culture medium containing 1% FBS. Transmigration of cells into the lower compartment containing 600 μl medium (9% FBS) occurred at 37 °C. After 24 h, transwells were removed and cleaned with cotton swabs to remove non-migrated cells. Migrated cells adherent to the bottom of the membrane were stained with crystal violet (Sigma-Aldrich). Each determination was done at least in duplicates. Data are expressed as the number of migrating cells per field. For invasion assays, the upper chambers were coated with matrigel before using and the procedures were as above.

For monolayer wound-healing assays, a total of 3×10^5 cells were collected and plated in a six-well plate. At 100% confluence, two parallel wounds of 1 mm were made using a pipette tip. The number of cells crawling into the wound was measured after 24 h, in three independent experiments.

Chromatin immunoprecipitation. Cells were cross-linked with 1% formaldehyde at room temperature for 10 min, washed twice with 10 ml ice-cold PBS, and then scraped into 0.5 ml of lysis buffer and left on ice for 10 min. Samples were treated according to the instructions of ChIP kit (Beyotime, Haimen, Jiangsu, China). Immunoprecipitations were performed overnight with GFI1 antibody (1–2 μg). Immune-complexes were captured by incubation with 40 μl protein A/G Sepharose. DNA extraction was performed using Qiagen Purification Kit. The samples were analysed by PCR using primers whose sequences are listed below.

STAT3 promoter-F: gggttagctgagcagtgacat
STAT3 promoter-R: aagctgataacgtgtagggct
PTGER2 promoter-F: gcgcattgtgtggtttggtt
PTGER2 promoter-R: acacagaagatcggggcaac

Animals. The DKO mice studies were approved by the Infection and Immunity Center of Chinese Academy of Sciences. DKO (BALB/c-*Rag2*$^{-/-}$*gc*$^{-/-}$) mice were kindly provided by Professor Lieping Chen, Department of Immunology, Yale University School of Medicine, New Haven USA and used at age of 8–12 weeks. The mice were maintained under specific pathogen-free conditions in the animal facility at the Institute of Biophysics, Chinese Academy of Sciences, Beijing, China. The female C57BL/6 mice were purchased from YISI Laboratory Animal Technology Co., Ltd. (Changchun, China) and used at 10-week-old. The female nude mice were purchased from Beijing Vital River Laboratory Animal Technology Co., Ltd. (Beijing, China) and used at 6-week-old. These mice were maintained under specific pathogen-free conditions in Infection Key Laboratory of Heilongjiang Province, Harbin, China.

Xenograft experiments. Approximately 1×10^7 HT29-NC and HT29-GFI1 cells pretreated with/without LSMCM for 24 h; or HT29-vector and HT29-shGFI1 cells were s.c. injected into the right flank of DKO or nude mice. Tumour growth was monitored every three days and tumour volumes were calculated by the equation V (mm^3) $= a\times b^2/2$, where *a* is the largest diameter and *b* is the perpendicular diameter.

Mouse *in vivo* metastasis studies. For *in vivo* metastasis assays, six-week-old DKO or nude mice were housed in a specific pathogen-free facility. In total, 7×10^6 human CRC cells were suspend in 100 μl culture medium and injected via the t.v. Mice were monitored every three days and body weights were measured. After 30, 40, or 60 d, mice were killed, and lungs and livers were collected and the metastases were counted and analysed, respectively.

For CRC liver metastasis models, 1×10^6 MC38 or MC38-Gfi1 cells were suspended in 100 μl culture medium and injected into spleen of 10-week-old C57BL/6 females. Part of animals were killed 16 d after cell injection and analysed.[60] Pathological changes were detected by H&E staining on the liver. The survival curves of the other part animals were analysed until 50 d or longer by GraphPad Prism Software.

Statistical analysis. Statistical analyses were performed using the GraphPad Prism Software. D'Agostino & Pearson normality test was performed prior to statistical analysis. For comparisons, Student's *t*-test (two-tailed) was used when normality test was achieved. Non-parametric test Mann–Whitney *U*-test was performed when normality test failed, Log-rank (Mantel–Cox) test was used for survival analysis, Pearson's correlation test was used to evaluate the expression relationships. A $P<0.05$ was considered significant.

Accession numbers. The mRNA expression data (TCGA, GSE17538, GSE41258, GSE14333 and GSE39582).

Conflict of Interest

The authors declare no conflict of interest.

Acknowledgements. We thank Dr Shoshana Yakar (New York University, USA) for kindly providing MC38 cell line. HT29-vector and HT29-shGFI1 cells were provided from Shenyang Bai Hao Biological Technology Co. Ltd. (Shen yang, China). This work is supported by grants from Natural Science Foundation of China (91229112, 30772238 and 81472367).

Author contributions

XW designed, analysed and interpreted the experiments and wrote the manuscript. XY helped with human data acquisition and analysis. LX and TL performed the lung metastasis model *in vivo* assays, Hematoxylin–eosin staining and

immunohistochemistry. EL and JW helped with the CRC liver metastasis models and reviewed the manuscript. ZH and JH performed the cell culture and CRC cell metastatic behaviour experiments. HX and HW performed the immunohistochemistry analysis and animal models. MK, LX., WS, XH and ZF assisted with data analysis and manuscript preparation. RH led the study, supervised the overall project and reviewed the manuscript. All authors reviewed and approved of the submitted manuscript.

1. Belcheva A, Irrazabal T, Robertson SJ, Streutker C, Maughan H, Rubino S *et al.* Gut microbial metabolism drives transformation of MSH2-deficient colon epithelial cells. *Cell* 2014; **158**: 288–299.
2. Gupta J, del Barco Barrantes I, Igea A, Sakellariou S, Pateras IS, Gorgoulis VG *et al.* Dual function of p38alpha MAPK in colon cancer: suppression of colitis-associated tumor initiation but requirement for cancer cell survival. *Cancer Cell* 2014; **25**: 484–500.
3. Katoh H, Wang D, Daikoku T, Sun H, Dey SK, Dubois RN. CXCR2-expressing myeloid-derived suppressor cells are essential to promote colitis-associated tumorigenesis. *Cancer Cell* 2013; **24**: 631–644.
4. Feagins LA, Souza RF, Spechler SJ. Carcinogenesis in IBD: potential targets for the prevention of colorectal cancer. *Nat Rev Gastroenterol Hepatol* 2009; **6**: 297–305.
5. Luo JL, Maeda S, Hsu LC, Yagita H, Karin M. Inhibition of NF-kappaB in cancer cells converts inflammation- induced tumor growth mediated by TNFalpha to TRAIL-mediated tumor regression. *Cancer Cell* 2004; **6**: 297–305.
6. Balkwill F, Charles KA, Mantovani A. Smoldering and polarized inflammation in the initiation and promotion of malignant disease. *Cancer Cell* 2005; **7**: 211–217.
7. Wang K, Karin M. Tumor-elicited inflammation and colorectal cancer. *Adv Cancer Res* 2015; **128**: 173–196.
8. Shalapour S, Karin M. Immunity, inflammation, and cancer: an eternal fight between good and evil. *J Clin Invest* 2015; **125**: 3347–3355.
9. Tan W, Zhang W, Strasner A, Grivennikov S, Cheng JQ, Hoffman RM *et al.* Tumour-infiltrating regulatory T cells stimulate mammary cancer metastasis through RANKL-RANK signalling. *Nature* 2011; **470**: 548–553.
10. Kim S, Karin M. Role of TLR2-dependent inflammation in metastatic progression. *Ann N Y Acad Sci* 2011; **1217**: 191–206.
11. Maeda S, Hikiba Y, Sakamoto K, Nakagawa H, Hirata Y, Hayakawa Y *et al.* Ikappa B kinasebeta/nuclear factor-kappaB activation controls the development of liver metastasis by way of interleukin-6 expression. *Hepatology* 2009; **50**: 1851–1860.
12. De Rosa M, Pace U, Rega D, Costabile V, Duraturo F, Izzo P *et al.* Genetics, diagnosis and management of colorectal cancer (Review). *Oncol Rep* 2015; **34**: 1087–1096.
13. Verma N, Keinan O, Selitrennik M, Karn T, Filipits M, Lev S. PYK2 sustains endosomal-derived receptor signalling and enhances epithelial-to-mesenchymal transition. *Nat Commun* 2015; **6**: 6064.
14. Hassan WA, Yoshida R, Kudoh S, Hasegawa K, Niimori-Kita K, Ito T. Notch1 controls cell invasion and metastasis in small cell lung carcinoma cell lines. *Lung Cancer* 2014; **86**: 304–310.
15. Calon A, Espinet E, Palomo-Ponce S, Tauriello DV, Iglesias M, Cespedes MV *et al.* Dependency of colorectal cancer on a TGF-beta-driven program in stromal cells for metastasis initiation. *Cancer Cell* 2012; **22**: 571–584.
16. Gasparini G, Longo R, Sarmiento R, Morabito A. Inhibitors of cyclo-oxygenase 2: a new class of anticancer agents? *Lancet Oncol* 2003; **4**: 605–615.
17. Wang D, Fu L, Sun H, Guo L, DuBois RN. Prostaglandin E2 promotes colorectal cancer stem cell expansion and metastasis in mice. *Gastroenterology* 2015; **149**: 1884–1895 e1884.
18. Ma X, Aoki T, Tsuruyama T, Narumiya S. Definition of prostaglandin E2-EP2 signals in the colon tumor microenvironment that amplify inflammation and tumor growth. *Cancer Res* 2015; **75**: 2822–2832.
19. Kaplan RN, Riba RD, Zacharoulis S, Bramley AH, Vincent L, Costa C *et al.* VEGFR1-positive haematopoietic bone marrow progenitors initiate the pre-metastatic niche. *Nature* 2005; **438**: 820–827.
20. von Karstedt S, Conti A, Nobis M, Montinaro A, Hartwig T, Lemke J *et al.* Cancer cell-autonomous TRAIL-R signaling promotes KRAS-driven cancer progression, invasion, and metastasis. *Cancer Cell* 2015; **27**: 561–573.
21. Xiao Y, Fan H, Zhang Y, Xing W, Ping Y, Zhao H *et al.* Systematic identification of core transcription factors mediating dysregulated links bridging inflammatory bowel diseases and colorectal cancer. *PLoS One* 2013; **8**: e83495.
22. Tili E, Michaille JJ, Wernicke D, Alder H, Costinean S, Volinia S *et al.* Mutator activity induced by microRNA-155 (miR-155) links inflammation and cancer. *Proc Natl Acad Sci USA* 2011; **108**: 4908–4913.
23. Grimes HL, Chan TO, Zweidler-McKay PA, Tong B, Tsichlis PN. The Gfi-1 proto-oncoprotein contains a novel transcriptional repressor domain, SNAG, and inhibits G1 arrest induced by interleukin-2 withdrawal. *Mol Cell Biol* 1996; **16**: 6263–6272.
24. Zeng H, Yucel R, Kosan C, Klein-Hitpass L, Moroy T. Transcription factor Gfi1 regulates self-renewal and engraftment of hematopoietic stem cells. *Embo J* 2004; **23**: 4116–4125.
25. Hock H, Hamblen MJ, Rooke HM, Schindler JW, Saleque S, Fujiwara Y *et al.* Gfi-1 restricts proliferation and preserves functional integrity of haematopoietic stem cells. *Nature* 2004; **431**: 1002–1007.
26. van der Meer LT, Jansen JH, van der Reijden BA. Gfi1 and Gfi1b: key regulators of hematopoiesis. *Leukemia* 2010; **24**: 1834–1843.
27. Zhu J, Guo L, Min B, Watson CJ, Hu-Li J, Young HA *et al.* Growth factor independent-1 induced by IL-4 regulates Th2 cell proliferation. *Immunity* 2002; **16**: 733–744.
28. Park JH, Yu Q, Erman B, Appelbaum JS, Montoya-Durango D, Grimes HL *et al.* Suppression of IL7Ralpha transcription by IL-7 and other prosurvival cytokines: a novel mechanism for maximizing IL-7-dependent T cell survival. *Immunity* 2004; **21**: 289–302.
29. Rodel B, Tavassoli K, Karsunky H, Schmidt T, Bachmann M, Schaper F *et al.* The zinc finger protein Gfi-1 can enhance STAT3 signaling by interacting with the STAT3 inhibitor PIAS3. *Embo J* 2000; **19**: 5845–5855.
30. Bjerknes M, Cheng H. Cell Lineage metastability in Gfi1-deficient mouse intestinal epithelium. *Dev Biol* 2010; **345**: 49–63.
31. Shroyer NF, Wallis D, Venken KJ, Bellen HJ, Zoghbi HY. Gfi1 functions downstream of Math1 to control intestinal secretory cell subtype allocation and differentiation. *Genes Dev* 2005; **19**: 2412–2417.
32. Fernandez-Pisonero I, Duenas AI, Barreiro O, Montero O, Sanchez-Madrid F, Garcia-Rodriguez C. Lipopolysaccharide and sphingosine-1-phosphate cooperate to induce inflammatory molecules and leukocyte adhesion in endothelial cells. *J Immunol* 2012; **189**: 5402–5410.
33. Harizi H, Limem I, Gualde N. CD40 engagement on dendritic cells induces cyclooxygenase-2 and EP2 receptor via p38 and ERK MAPKs. *Immunol Cell Biol* 2011; **89**: 275–282.
34. Guo RX, Qiao YH, Zhou Y, Li LX, Shi HR, Chen KS. Increased staining for phosphorylated AKT and nuclear factor-kappaB p65 and their relationship with prognosis in epithelial ovarian cancer. *Pathol Int* 2008; **58**: 749–756.
35. Williams TM, Leeth RA, Rothschild DE, Coutermarsh-Ott SL, McDaniel DK, Simmons AE *et al.* The NLRP1 inflammasome attenuates colitis and colitis-associated tumorigenesis. *J Immunol* 2015; **194**: 3369–3380.
36. Foersch S, Sperka T, Lindner C, Taut A, Rudolph KL, Breier G *et al.* VEGFR2 signaling prevents colorectal cancer cell senescence to promote tumorigenesis in mice with colitis. *Gastroenterology* 2015; **149**: 177–189 e110.
37. Sica GS, Fiorani C, Stolfi C, Monteleone G, Candi E, Amelio I *et al.* Peritoneal expression of Matrilysin helps identify early post-operative recurrence of colorectal cancer. *Oncotarget* 2015; **6**: 13402–13415.
38. Noy R, Pollard JW. Tumor-associated macrophages: from mechanisms to therapy. *Immunity* 2014; **41**: 49–61.
39. Yiakouvaki A, Dimitriou M, Karakasiliotis I, Eftychi C, Theocharis S, Kontoyiannis DL. Myeloid cell expression of the RNA-binding protein HuR protects mice from pathologic inflammation and colorectal carcinogenesis. *J Clin Invest* 2012; **122**: 48–61.
40. Biswas S, Trobridge P, Romero-Gallo J, Billheimer D, Myeroff LL, Willson JK *et al.* Mutational inactivation of TGFBR2 in microsatellite unstable colon cancer arises from the cooperation of genomic instability and the clonal outgrowth of transforming growth factor beta resistant cells. *Genes Chromosomes Cancer* 2008; **47**: 95–106.
41. Grivennikov SI, Greten FR, Karin M. Immunity, inflammation, and cancer. *Cell* 2010; **140**: 883–899.
42. Igwe E, Kosan C, Khandanpour C, Sharif-Askari E, Brune B, Moroy T. The zinc finger protein Gfi1 is implicated in the regulation of IgG2b production and the expression of Igamma2b germline transcripts. *Eur J Immunol* 2008; **38**: 3004–3014.
43. Yang J, Weinberg RA. Epithelial-mesenchymal transition: at the crossroads of development and tumor metastasis. *Dev Cell* 2008; **14**: 818–829.
44. Voronov E, Shouval DS, Krelin Y, Cagnano E, Benharroch D, Iwakura Y *et al.* IL-1 is required for tumor invasiveness and angiogenesis. *Proc Natl Acad Sci USA* 2003; **100**: 2645–2650.
45. Wu Y, Deng J, Rychahou PG, Qiu S, Evers BM, Zhou BP. Stabilization of snail by NF-kappaB is required for inflammation-induced cell migration and invasion. *Cancer Cell* 2009; **15**: 416–428.
46. Zhang Y, Sime W, Juhas M, Sjolander A. Crosstalk between colon cancer cells and macrophages via inflammatory mediators and CD47 promotes tumour cell migration. *Eur J Cancer* 2013; **49**: 3320–3334.
47. Solinas G, Schiarea S, Liguori M, Fabbri M, Pesce S, Zammataro L *et al.* Tumor-conditioned macrophages secrete migration-stimulating factor: a new marker for M2-polarization, influencing tumor cell motility. *J Immunol* 2010; **185**: 642–652.
48. Wang S, Liu Z, Wang L, Zhang X. NF-kappaB signaling pathway, inflammation and colorectal cancer. *Cell Mol Immunol* 2009; **6**: 327–334.
49. Klampfer L. The role of signal transducers and activators of transcription in colon cancer. *Front Biosci* 2008; **13**: 2888–2899.
50. Terzic J, Grivennikov S, Karin E, Karin M. Inflammation and colon cancer. *Gastroenterology* 2010; **138**: 2101–2114, e2105.
51. Taniguchi K, Karin M. IL-6 and related cytokines as the critical lynchpins between inflammation and cancer. *Semin Immunol* 2014; **26**: 54–74.
52. Polytarchou C, Hommes DW, Palumbo T, Hatziapostolou M, Koutsioumpa M, Koukos G *et al.* MicroRNA214 is associated with progression of ulcerative colitis, and inhibition reduces development of colitis and colitis-associated cancer in mice. *Gastroenterology* 2015; **149**: 981–992.
53. Castellone MD, Teramoto H, Gutkind JS. Cyclooxygenase-2 and colorectal cancer chemoprevention: the beta-catenin connection. *Cancer Res* 2006; **66**: 11085–11088.
54. Aggarwal BB, Shishodia S, Sandur SK, Pandey MK, Sethi G. Inflammation and cancer: how hot is the link? *Biochem Pharmacol* 2006; **72**: 1605–1621.
55. Chen WS, Wei SJ, Liu JM, Hsiao M, Kou-Lin J, Yang WK. Tumor invasiveness and liver metastasis of colon cancer cells correlated with cyclooxygenase-2 (COX-2) expression and inhibited by a COX-2-selective inhibitor, etodolac. *Int J Cancer* 2001; **91**: 894–899.

56. Zhang XH, Jin X, Malladi S, Zou Y, Wen YH, Brogi E *et al.* Selection of bone metastasis seeds by mesenchymal signals in the primary tumor stroma. *Cell* 2013; **154**: 1060–1073.
57. Klein CA. Selection and adaptation during metastatic cancer progression. *Nature* 2013; **501**: 365–372.
58. Dupaul-Chicoine J, Arabzadeh A, Dagenais M, Douglas T, Champagne C, Morizot A *et al.* The Nlrp3 inflammasome suppresses colorectal cancer metastatic growth in the liver by promoting natural killer cell tumoricidal activity. *Immunity* 2015; **43**: 751–763.
59. Vanharanta S, Massague J. Origins of metastatic traits. *Cancer Cell* 2013; **24**: 410–421.
60. Sanchez-Lopez E, Flashner-Abramson E, Shalapour S, Zhong Z, Taniguchi K, Levitzki A *et al.* Targeting colorectal cancer via its microenvironment by inhibiting IGF-1 receptor-insulin receptor substrate and STAT3 signaling. *Oncogene* 2015; **35**: 2634–2644.

Supplementary Information accompanies this paper on Cell Death and Differentiation website (http://www.nature.com/cdd)